The Mass and Mass-to-Light Ratio for Clusters of Galaxies at Large Radii

Henrik Vedel

Theoretical Astrophysics Center, Juliane Maries Vej 30,
DK-2100 Copenhagen, Denmark

F.D.A. Hartwick

Dept. of Physics & Astronomy, P.O. Box 3055, University of Victoria
Victoria, B.C. V8W 3P6, Canada

e-mail: vedel@tac.dk and hartwick@uvastro.phys.uvic.ca

ABSTRACT

We construct models describing the velocity field in the infall regions of clusters of galaxies. In all models the velocity field is the superposition of a radial systematic component which is assumed spherically symmetric, and a "noise" component of random nature. The latter accounts for the combined effects of small-scale substructure and observational errors. The effect of the noise term is to smear out the caustic envelopes searched for by previous groups, resulting in models which resemble the observations quite well. When the systematic component is known, the infall velocity and the mass profile of the infall region of the clusters can be determined.

Given a particular model, it is possible to calculate the distribution function, $f(cz, \theta, m)$, at all points in the observable (cz, θ, m)-phase-space outside the virialized region. It is demonstrated, on simulated data, that the use of a maximum-likelihood estimator enables identification of the correct model, even at realistic noise levels. To minimize systematic effects due to deviations from spherical infall, observations from a number of clusters should be used when applying the method to a real dataset. Combining data from different clusters is a straight-forward procedure.

In the models the mass-to-light ratio is allowed to vary freely with radius. Furthermore, the models do not require any knowledge of the virial region. Rather, such knowledge can be used to test the models ability to produce realistic results by comparing the mass estimated by the models at small radii to the mass estimates obtained for the inner region using the virial theorem.

As a corollary we show how distance information of the quality obtained using the Tully-Fisher relation enhances the likelihood signal. Such distance information might be used in the future to either strengthen the results for this type of model or allow more advanced models to be used (e.g. models breaking the assumption of spherical symmetry).

The method relies on observations of redshifts of galaxies at large angular separations from the centers of the clusters. Currently such data exist only for Coma, to which we apply the method as an example. The estimated mass at $r = 2.5h^{-1}Mpc$ falls in the range $1.1 - 2.4 \times 10^{15}h^{-1}M_{\odot}$, depending on the model and the level of the noise term. We find r_{turn} to be of the order $10h^{-1}Mpc$, a result which is rather robust against changes in the model and subdivision of the data in various ways. We find $0.6 < \frac{\Omega_0^{0.6}}{b^{0.75}} < 0.8$, where b is the bias parameter, when using the luminosity profile adopted in the models. Interpreting this result one must recall that the luminosity function of Coma is not well known in the infall region, and that ideally the method should be used on several clusters simultaneously to minimize the effects of deviations from the spherical model.

The method provides a promising way of measuring the infall velocities in the outer regions of clusters. However, a robust determination of cluster properties must await future redshift observations of galaxies in the outer regions of a number of clusters.

Subject headings: galaxies: clustering — clusters: mass, mass-to-light ratios

1. INTRODUCTION

Current estimates of Ω_0 based on the mass-to-light ratio found for the virialized central regions of clusters of galaxies favour a low value (Carlberg et al. 1997a, David, Jones, & Forman 1995, Tyson & Fisher 1995, Squires et al. 1996, Smail et al. 1997, Fisher & Tyson 1997), of the order $\Omega_0 \approx 0.25$. Estimates from much larger scales often favour higher values, including $\Omega_0 = 1$, but the uncertainties are in general rather large (see Dekel, Burstein, & White 1996 for a recent review).

If the global value of M/L is significantly higher than the value found for the central parts of clusters it would not be unnatural for the change to manifest itself in the infall region of the clusters. If, for example, the difference is due to environmental effects resulting in the baryons being "lit up" depending on the properties of the surroundings, one can argue that the infalling galaxies formed well away from the clusters and have yet to be strongly affected by cluster imposed tidal fields, hot cluster gas, etc. Furthermore numerical simulations indicate that the extent of the mass density profiles of clusters is related to Ω_0, more extensive profiles corresponding to higher values of Ω_0 due to ongoing infall (Crone, Evrard, & Richstone 1994). The steepness is also related to the precise form of the initial spectrum of density fluctuations, however.

Obtaining mass profiles of the outer regions of clusters is therefore highly relevant.

Three main measures are being used for determination of the mass-to-light ratio of clusters: the velocity dispersion, the temperature of the hot X-ray emitting gas in the clusters, and the distortion of the shapes of background galaxies. The first two rely on the assumption of virial equilibrium and are consequently not the ideal tools for a determination of the mass at significantly larger radii than the virial radius, at least not without some modification of the approach governed by insight from N-body simulations. Observation of weak gravitational lensing using new 8–10-m telescopes and large array CCDs is a very promising technique which potentially can probe the cluster potentials far into the infall region. However, at present the mass estimates found from the weak lensing method generally apply to the inner regions.

In this paper we shall develop a second method; we attempt to measure the systematic part of the velocity field of the galaxies in the infall region.

As the peculiar velocities, relative to those expected for a pure Hubble flow, will be larger near a cluster than in the general field one might expect it to be a less difficult task to map the peculiar velocity field of the galaxies surrounding a cluster rather than the velocity field on scales on which linear theory applies. However, even though the infall signal should be rather strong , projection effects and our inability to measure distances of

galaxies precisely makes the determination difficult.

Kaiser (1987) applied the spherical infall model (e.g. Lilje & Lahav 1991) to an (adopted) spherical cluster density profile and found that it manifest itself as a characteristic diamond shaped distribution in the distribution of galaxies in the (cz, θ)-plane due to caustics. (here cz is the redshift and θ is the angular separation between a given galaxy and the cluster center).

Regös & Geller (1989, RG) extended the work of Kaiser and showed that the shapes and sizes of the caustics are a characteristic of the mass enclosed. RG assumed light to trace mass, in which case Ω_0 becomes the only free parameter of the model, as the observed luminosity profile can be deconvolved and used to deduce the relative mass over-density as a function of radius. Fitting their models by eye to observations of the Coma-cluster (and a few other clusters) RG were not able to put new constraints on Ω_0, however. The data available to them were limited, and what they had appeared to be more noisy than predicted by their models. The density gradients across the caustics seemed to be weaker than predicted by their model.

Van Haarlem et al. (1993, vH) adopted the basic assumptions of RG and refined their work on the Coma cluster in three ways: Firstly, they introduced an objective measure of the change in density between the region just inside and just outside the position of the caustics predicted by a given model, allowing a more rigorous fitting procedure. Using Monte Carlo simulated artificial clusters the new measure was shown to work well. Secondly they extended the number of observations available by performing a small redshift survey around the Coma cluster for $\theta[1°; 3°]$, adding 98 new redshifts to the Coma sample. Thirdly, using scans of Schmidt plates, they determined the luminosity profile of Coma as well as is currently possible (assuming spherical symmetry).

Despite this the result was still inconclusive, which they noted was due to the caustics being smeared out in the observational sample, whereas the model caustics were very sharp. vH attributed the smearing observed in real clusters to a non-spherical mass distribution, and they demonstrated that an ellipsoidal mass distribution will produce a distinct smearing of the infall in the (cz, θ)-plane. Later work (e.g. van Haarlem & van de Weygaert 1993), show the non spherical distribution of the infalling material (infall along filaments), and the event-like nature of part of the infall, to be important factors, however.

In this paper we show that keeping the spherical approximation for the infall, but adding noise to the models, noise which is known to exist in all clusters, and which represents the combined effects of the velocities induced by small scale density fluctuations and observational errors, can be responsible for much of the smearing of the caustics. We

are able to produce artificial clusters with our models which appear quite like real clusters in the (cz, θ)-plane.

The organisation of the paper is as follows: Section 2 describes the models, the maximum likelihood procedure used to fit models to data, and tests of the procedure on simulated data. In Section 3 the models are applied to the Coma cluster as an example. Section 4 contains a discussion of our findings and assumptions, and Section 5 the conclusions.

2.   MODELS AND TESTS OF MODELS

We will construct models which allow us to determine the infall velocity profile and mass profile of clusters of galaxies beyond the virial region, based upon observations of the position on the sky, the line-of-sight velocity, and the magnitudes of individual galaxies in and around the clusters.

We shall attempt to perform this task by first constructing a series of simple models of the velocity field of the region beyond the distance of shell crossing, with each model having only a few free parameters to be determined. Secondly, the distribution function, $f(cz, \theta, m)$, which expresses the number density of galaxies expected at any given point in the observed region of phase-space is calculated for each model. Finally, the best-fitting parameters are found using maximum-likelihood techniques.

With the model-parameters in hand, estimates of the basic properties of the outer regions of a cluster, such as the mass inside a given radius, the mass-to-light ratio (M/L), and the turn-around radius can be estimated, and eventual conclusions about Ω_0 can be drawn.

In all of the following we define the "infall region" as the region of a cluster which is *outside* the part seriously effected by processes associated with virialization and shell crossing and *inside* the volume outside which neighbouring clusters have a significant impact on the peculiar velocities of the galaxies relative to those induced by the cluster itself. We shall apply our models only to the infall region, as here defined. It contains galaxies which are falling towards the cluster for the first time as well as more distant galaxies which are still moving away from the cluster.

We shall assume that the velocity field in the infall region can be adequately described by a systematic component which is the one we want to determine plus a 'noise' component of random nature. The latter allows for the effects of substructure, non-radial motions, and

observational errors.

Following RG, we will let the systematic component of the velocity field be given by a spherically symmetric radial flow. Many clusters show evidence for deviations from spherical flow, but combining data from a number of clusters we expect the effects of non-sphericity to be minimized out, resulting in a spherical cluster while adding some extra noise to the infall signal.

2.1.   Infall Velocity Versus Density in the Spherical Approximation

The spherical approximation is based on the constraint that one is dealing with a spherically symmetric density fluctuation and the corresponding purely radial velocity fluctuation in an otherwise perfectly homogeneous and isotropic background universe. In the limit of no shell crossings (i.e. there is no mass transport through the shell over the time span considered) the evolution of the radius of a shell and the current time are related through the following equations:

$$\frac{r}{r_i} = \frac{a}{|b|}f(\eta) \quad \text{and} \quad tH_0 = \frac{a}{|b|^{3/2}}g(\eta), \tag{1}$$

where:

$$f(\eta) = \begin{cases} 1 - \cos\eta, & b > 0 \\ \cosh\eta - 1, & b < 0 \end{cases} \quad \text{and} \quad g(\eta) = \begin{cases} \eta - \sin\eta, & b > 0 \\ \sinh\eta - \eta, & b < 0 \end{cases}, \tag{2}$$

where a, b, r_i are constants related to the initial properties of the shell and to the type of cosmology (e.g. Peebles 1980). Throughout this paper we use $100hMpc$ km^{-1} s^{-1} for the value of the Hubble constant H_0.

It follows that the ratio of today's velocity, $v(r)$, of a given shell at distance r from the center of the perturbation to the velocity difference expected over the same distance in a situation with pure Hubble flow is:

$$\frac{v}{H_0 r} = \frac{1}{t_0 H_0} \frac{g(\eta)f'(\eta)}{f^2(\eta)}, \tag{3}$$

whereas the ratio of today's mean density inside the same shell, $\overline{\rho}(r)$, to that of the background universe is given by:

$$\frac{\overline{\rho}}{\rho_0} = \frac{2}{(t_0 H_0)^2 \Omega_0} \frac{g^2(\eta)}{f^3(\eta)}, \tag{4}$$

(e.g. Silk 1977). Remembering that:

$$t_0 H_0 = \begin{cases} \frac{1}{1-\Omega_0} - \frac{\Omega_0}{2(1-\Omega_0)^{2/3}}\cosh(\frac{2}{\Omega_0} - 1), & \Omega_0 < 1 \\ \frac{2}{3}, & \Omega_0 = 1, \end{cases} \tag{5}$$

and
$$\rho_0 = \frac{3\Omega_0 H_0^2}{8\pi G} \tag{6}$$
it is possible to determine the mass profile in the infall region of a cluster if one can somehow measure its velocity profile. When combined with the luminosity profile of the cluster, M/L can be determined.

Unfortunately, it is currently not possible to measure the line-of-sight velocity as a function of distance directly, from which $v(r)$ could be obtained. Distance estimates for galaxies are far from being precise enough. One is forced to work primarily with angular position plus redshift data, and consequently $v(r)$ must be obtained in a much more indirect way.

In this work we do so by constructing a model which predicts the distribution of cz as a function of θ on the basis of assumed functional forms of $v(r)$, and subsequently we fit the distribution to the data obtaining a best-fitting $v(r)$.

2.2. Models of the Systematic Component

It is non-trivial to write down the mass or velocity profile expected for the infall region. Most of our current knowledge about the density and velocity profiles of clusters comes from the inner regions. This is true both for observational and theoretical work (including N-body simulations). Simply extrapolating those profiles out to the infall region might lead to biased results. In the absence of knowledge of the actual profile, we have found it important to use a number of different model profiles in order to make sure the results obtained are not just artifacts of our ignorance.

The adopted profiles should contain as few free parameters as possible, given the currently meager amount of observational data, the likely effects of the deviations between our spherical approach and reality, and the level of "noise terms" which smear out the clean signal of $v(r)$.

In terms of the ratio of the radial velocity relative to that expected for a pure Hubble flow at the same distance, $H(r) \equiv v(r)/(H_0 r) = 1 - v_{peculiar}(r)/(H_0 r)$, the first two of our adopted velocity profiles can be written as:
$$H = 1 - (\frac{r}{r_{turn}})^{-\beta} \tag{7}$$
$$H = 1 - \beta \exp(-\frac{r}{r_{turn}} \log \beta), \tag{8}$$
with each of them containing two free parameters which must be estimated.

Two additional profiles were given by specifying the average mass-density profile as a function of cluster-centric radius:

$$\frac{\overline{\rho}}{\rho_0} = 1 + (\frac{\overline{\rho}(r_{turn})}{\rho_0} - 1)(\frac{r}{r_{turn}})^{-\gamma} \tag{9}$$

$$\frac{\overline{\rho}}{\rho_0} = \frac{\overline{\rho}(r_{turn})}{\rho_0}(\frac{r}{r_{turn}})^{-\gamma}. \tag{10}$$

For future reference we label the above four models VI, VII, DI, and DII, respectively.

As we have seen, for a given value of Ω_0 and H_0 there is a one-to-one correspondence between a velocity profile and a mass profile. Working directly with a velocity profile emphasizes the fact that determination of the infall pattern can be considered a purely empirical task. Furthermore, it can be done independently of Ω_0. However, for certain combinations of the fitting parameters, the assumed profiles correspond to unphysical situations. The local density inferred from the velocity profile may become negative at certain radii within the region considered. It is straight forward to identify the subsets of parameters which correspond to unphysical situations, but we shall not pursue the point any further in this paper. Here we present the method rather than a determination of real cluster parameters.

The profiles VI, VII, and DI all approach a pure Hubble flow at large distances, whereas the profile DII does not. Profile DII corresponds to a situation in which the surroundings of the clusters have a lower mass-density than the universal average. However, as we consider only the region near the cluster, one should see the inclusion of profile DII rather as an attempt to check what will happen if the density is allowed to vary significantly around the turn-around radius, rather than be forced to go smoothly towards the background density at the turn-around radius. While the VI profile corresponds to a faster infall at smaller radii, as expected for a "pure" infall situation, the VII profile reaches a minimum at a certain radius and then approaches zero as the radius decreases. The latter is in accordance with the behaviour found in N-body simulations, where (more or less by definition) the radial velocity is zero in the virial core of the cluster and is followed by a transition zone which can stretch outside the virial radius (see Figure 5 of Crone et al. 1994). We expect profile VII to be less sensitive to a misplacement of the inner cutoff in the data sample, should the cutoff be done at too small an angular separation. On the other hand, one can obviously not use the part of the VII profile inside the minimum to determine a density profile for the cluster, as it becomes difficult to judge how smoothly the mass estimate produced using the infall profile joins the mass estimate of the inner, virialized part of the cluster using profile VII.

2.3. The Distribution Function Corresponding to Purely Systematic Infall

Using Figure 1 to define our coordinates, an observer located at a distance R from the cluster would find the line-of-sight velocity of a galaxy located at (θ, s) to be (RG):

$$v_{los} \equiv cz = H_0 R \{\cos\theta + (\frac{s}{R} - \cos\theta)H\}, \tag{11}$$

Let the spatial number-density of galaxies be $n_{gal}(r)$, the number of galaxies found in a small portion of the (cz, θ)-plane then becomes:

$$n(cz, \theta)dczd\theta = n_{gal}(r)s^2 \sin\theta |{\rm J}|^{-1}dczd\theta, \tag{12}$$

where:

$$\mathrm{J} = \begin{vmatrix} \frac{\partial cz}{\partial s} & \frac{\partial \theta}{\partial s} \\ \frac{\partial cz}{\partial \theta} & \frac{\partial \theta}{\partial \theta} \end{vmatrix} = \frac{H_0 R}{r}\{(\frac{s}{R} - \cos\theta)^2 \frac{\partial H}{H_0 \partial r} + \frac{H}{H_0}\frac{r}{R}\} \tag{13}$$

is the Jacobian of the transformation between the two coordinate systems. This result was presented by RG (to within a typographical error). Zero points in $J^{-1}(cz, \theta)$ make the distribution $n(cz, \theta)$ have a very characteristic "horn" shape. Although n naturally has to be integratable over a finite volume of phase-space, the high-density regions around these caustic surfaces do contain enough material for the surfaces to be easily recognisable even in a modest dataset (Figure 2a). Such a profile was noted by Kaiser (1987) and RG, and its use as a promising way of determining the infall velocities and enclosed masses as a function of radius has been investigated (RG, vH).

However, a number of effects complicate the situation making a direct identification of the "horn" almost impossible in a set of real observational data. In most clusters only a small number of galaxies have been observed within the infall region. A dedicated observational program can change this picture for the better, but clusters contain a finite number of galaxies and identifying the "horn" may demand combining data for a number of clusters, even if every galaxy in the infall region has a measured redshift. Secondly, the velocity field is probably not perfectly radial, even in the region dominated by infall, as envisaged by the various degrees of substructure on small and intermediate scales seen in many clusters. That will tend to smear out the caustics (vH), as will observational errors in the redshifts. In the next section we shall include a term in the models which incorporates the effects of small-scale substructure and observational errors.

2.4. Inclusion of the Noise Term

Within the hierarchical picture of structure formation the dynamical time scales for the evolution of small-scale structures (galaxies and groups) are generally shorter than for

larger scales (clusters); a difference increasing if the power spectrum describing the initial density fluctuations on those scales becomes steeper. When the dynamical time scales are sufficiently different, the internal dynamics of pairs and groups of galaxies in the infall region can be considered independent of the slower formation of the cluster. If so, the effect of small-scale substructure on the velocity field of the infall region of a cluster will be isotropic and independent of the position of the galaxies with respect to the cluster. We shall assume this to be the situation, in which case a rough estimate of the effects of small-scale structure can be obtained by folding the distribution with a Gaussian smearing function, $G(x, \sigma) = 1/(\sqrt{2\pi}\sigma)\exp(-0.5x^2/\sigma^2)$, leading to:

$$n_{\sigma_{cz}}(cz, \theta) = \int_{-\infty}^{+\infty} n(cz, \theta')G(cz' - cz, \sigma_{cz})dcz' \tag{14}$$

$$= \int_{-\infty}^{+\infty} n_{gal}(r[\theta, s'])G(cz[\theta, s'] - cz, \sigma_{cz})s'^2 \sin\theta ds', \tag{15}$$

the latter being the form most easily handled in numerical calculations for relevant values of σ_{cz}.

The observational data consist of inhomogeneous datasets obtained using different selection functions. In general, however, the selection functions are much nearer to being magnitude limited rather than volume limited, and we have to include the depth effect, at least for clusters as near as Coma.

Let $n_L(M)$ be the luminosity distribution of galaxies, and assume n_L is independent of the position (within the infall region) relative to the cluster position. If the sample is magnitude limited, we can write the proper distribution function as:

$$n_{\sigma_{cz}}(cz, \theta, m) = \int_{-\infty}^{+\infty} n_{gal}(r[\theta, s'])G(cz[\theta, s'] - cz, \sigma_{cz})n_L(M[m, s'])s'^2 \sin\theta ds' \tag{16}$$

and $M(m, s) = m - 25 - 5log_{10}s$, with m and M being apparent and absolute magnitudes, respectively.

This is our final distribution function. We shall now test its ability to infer correct parameters on simulated clusters, but first we demonstrate the effect of σ_{cz}. Figures 2a–2c show the distribution in the (cz, θ)-plane with and without the noise term included. The improvement from adding the noise term is quite evident, when compared to a real case as in Figure 2b (Coma). Figure 3 shows the number density along a line-of-sight for various degrees of smearing. Figures 2a, 2c, and Figure 3 were constructed using profile VI, $\beta = 1.4$, and $r_{turn} = 9Mpc$.

Which value should be used for σ_{cz}? There are not enough data to allow σ_{cz} to be a free parameter in the models. Rather, we find guidance from the observed pairwise velocity

dispersion (reduced to that of a single galaxy) at small scales. Unfortunately, there is no current consensus as to the proper level of the pairwise velocity dispersion. The recent determination by Markze et al. (1995) found $\sigma_{1-2} = 540$ km s^{-1}, markedly higher than the previous value, $\sigma_{1-2} = 340$ km s^{-1}, found by Davis & Peebles (1977). However, as shown by Markze et al. (1995), σ_{1-2} is strongly influenced by the fraction of highly clustered galaxies included in a sample, as these galaxies, despite being relatively few, have a significant effect through their large relative velocities. Removing all Abell clusters of richness class $R \geq 1$, they find $\sigma_{1-2} = 295$ km s^{-1}. This could argue for the use of a low value. However, the current neglect of non-spherical effects and the future extra noise from superposition of a number of clusters calls for a value somewhat above the estimate from pairwise velocity dispersions. Currently we bracket the problem by using the two values, $\sigma_{cz} = 300$ km s^{-1} and $\sigma_{cz} = 400$ km s^{-1}.

In the above calculations we have adopted $n_{gal}/n_0 = 1 + \xi_{cg}$, with $\xi_{cg} = (r/r_c)^{-\gamma}$ being the cluster-galaxy correlation function and using $\gamma = 2.5$ (Lilje & Efstathiou 1988), n_0 is the mean number-density of galaxies in the Universe. Whereas this is a natural choice in cases where little is known about the number density profile of the cluster in question, other choices are of course possible, e.g. using the observed (deconvolved) profile – though one should notice that it is very difficult to determine the luminosity profile of a single cluster in the region considered here. We have experimented using different parameterizations of $n_{gal}(r)$. Fortunately, it turns that the method is rather insensitive to these changes.

2.5.   Fitting a Model to the Data

We fit the models to the data by maximising the expression:

$$\ln \mathrm{L}(\text{model}) = \sum_{i=1}^{N} \ln p(cz_i, \theta_i, m_i | \text{model}), \tag{17}$$

where:

$$p(cz, \theta, m | \text{model}) \equiv \frac{n_{\sigma_{cz}}(cz, \theta, m)}{\int \int \int n_{\sigma_{cz}}(cz', \theta', m')dcz'd\theta'dm'} \tag{18}$$

is the probability of observing a galaxy at (cz, θ, m), given a particular model and its parameters, and the integral is over the region of phase space from which the data are drawn. N is the total number of galaxies in the sample.

This procedure is superior to envelope fitting of the caustics, as all data points contribute to the fit, thereby making the most of the available information. Due to the inclusion of the noise term, $p(cz_i, \theta_i, m_i | \text{model})$ is a rather gently changing function in cz,

and in practice it turns out not to be necessary to discretize $p(cz, \theta, m)$ in θ or cz before calculating L, even for rather small data samples. One should check, however, that no galaxies of highly unusual brightness for a sample of a given size and distance are included when fitting, as such a galaxy can have a large impact on the results. Such a galaxy should either be excluded or $p(cz, \theta, m)$ has to be discretized with respect to magnitude.

An important, valuable feature of the model is the fact that it is not necessary to correct for foreground and background objects, as they are included in the model. This is not the case for members of neighbouring clusters however, and care should therefore be taken to select data from a region of phase-space surrounding each cluster which is small enough that nearby clusters will only have a minor effect on the velocities. On the other hand, in the absence of neighbour problems, the method produces better determinations of the model parameters when the cuts in cz are sufficiently widespread to include the caustics at all selected θ, and the cuts in θ are wide enough to cover the whole region between the radius of no shell crossing and r_{turn}. In each case one has to weigh these arguments and find a working compromise.

2.6.   Testing the Procedure on Simulated Clusters

Previously we demonstrated that the inclusion of a noise term in the spherical infall model and a few further reasonable assumptions produce simulated clusters which 'to the eye' mimic real clusters quite well (Figure 2).

We shall now test our maximum-likelihood estimator, by using it on simulated clusters in order to evaluate whether it is capable of identifying the correct parameters at all (recalling that the previous attempts to identify caustics for real clusters failed). If so, what is its sensitivity and how big are the errors arising from assuming wrong model parameters for a given type of cluster?

We have performed numerous tests on simulated clusters for which all model parameters were known. In most cases the simulated clusters contained 143 galaxies (sometimes 286) chosen randomly according to the distribution function $p(cz, \theta, m|model)$ (Equation 18) and having $2 < \theta < 8$, 4930 km s^{-1} $< cz <$ 8930 km s^{-1}, a cluster-centric velocity of 6930 km s^{-1}, $\gamma_{cg} = 2.5$, and a magnitude cutoff at 15.5. These parameters may appear odd, but they correspond to those of our prime sample of real data (Coma).

The results are presented in Table 1a. In the table, column 1 indicates the systematic component with which the simulated clusters were made, column 2 gives the velocity dispersion used in the smearing function of the simulated clusters, columns 3 and 4 give

the systematic component and the velocity dispersion assumed when doing the likelihood analysis, column 5 is the number of simulated clusters on which the analysis was done, column 6 gives the average value of r_{turn} and its dispersion from the maximum-likelihood analysis, and column 7 gives the average value of β (or γ for the density profile models) and its dispersion. All simulated clusters made using the profile VI were given parameters: $(r_{turn}, \beta) = (9, 1.4)$, using VII: $(r_{turn}, \beta) = (9, 8)$, and using DI: $(r_{turn}, \gamma) = (9.5, 2.5)$.

First we note that the adopted maximum-likelihood technique is indeed able to return the proper parameters, even for σ_{cz} as high as 400 km s^{-1}. As might be expected the precision depends on σ_{cz}, the match between the model assumed for the simulated cluster (reality), and the model used for analysis. However, even in cases of mis-match or high σ_{cz} the results are still reasonable.

Figure 4 gives an example of a contour plot for the maximum-likelihood levels found for a random simulated cluster ($\sigma_{cz} = 300$ km s^{-1}). The plot shows $\ln(L)$, the cross identifies the position of maximum-likelihood, and the levels are separated by $\ln(2)$ and constantly decreasing as one gets farther from the peak. There is some degree of degeneracy between r_{turn} and γ (and similarly for velocity profile models between r_{turn} and β). This reflects the fact that for certain correlated changes of (r_{turn}, γ) the corresponding changes in the velocity profile (and density profile) are rather small. The uncertainty of an individual "measurement" in some cases is rather large, and ideally a number of clusters should be used when determining model parameters for a set of real data.

2.7. Extension of the Model to Include Distance Information

Obviously one cannot determine the parameters of an infall profile, $v(r)$ without knowledge of both v and r. In the model above that information comes about rather indirectly in the form of distribution functions calculated on the basis on an assumed profile $v(r)$ (and other model parameters) and the observed values of cz and θ. Due to the existence of multiple solutions for the distance for certain combinations of (cz, θ) even without noise, and due to the assumption of a random scatter in cz of the order $\sigma_{cz} \geq 300$ km s^{-1}, the probability distribution, $p(s|cz, \theta, m)$, of galaxy being at a particular distance given the observed (cz, θ, m) is very broad. For most galaxies it is even impossible to tell whether they are in front of or behind the cluster. But as has been demonstrated it is still possible to reliably estimate the parameters of the infall profile.

It seems worthwhile to test whether use of observed distances leads to an improved determination of the model parameters, even though the uncertainty in distance estimate

for galaxies is at present quite considerable relative to the sizes of the clusters in question. (If that was not the case the whole procedure presented in the previous sections clearly becomes obsolete, and one could do much better using another approach.)

Therefore, assume that for a given distance estimator the probability that a galaxy of true magnitude M_t and inferred magnitude M_o is given by $G(M_o - M_t, \sigma_m)$. For the Tully-Fisher relation σ_m is of the order 0.38 (c.f. Willick et al. 1997). With s being the true distance, the probability of observing a galaxy at distance s_o becomes:

$$p(s_o|s) = \frac{5}{\ln 10\sqrt{2\pi}\sigma_m} \frac{1}{s_o} e^{-\frac{25log_{10}^2(s_o/s)}{2\sigma_m^2}}. \tag{19}$$

Including this term in the expression for $n(cz, \theta, m)$ (Equation 16 and further) provides a simple way of including the distance information in the likelihood estimates. (As the above expression is already normalized and does not depend on model parameters other than σ_m, the extra integration over s_o in the normalization of $n(cz, \theta, m, s_o)$ is trivial as long as no cuts are made in s_o space when selecting the sample.)

Table 1b shows the result of including distance information in the tests on simulated clusters. Except for the added distance information (assuming $\sigma_m = 0.38$) for the simulated clusters and the inclusion of the distance term in the distribution function used in the maximum-likelihood analysis, everything is performed exactly as outlined in the previous sections, including the format of the table. Clearly distance information has a significant impact even for realistic values of σ_m. It would be of great value to have distances for the galaxies which are to be used in deriving infall profiles, despite the $\sim$20% uncertainty of a single distance measurement. It is not clear whether the best observing strategy is to start measuring more distances to galaxies in the infall regions of a few clusters or to measure many more redshifts of galaxies in a larger number of clusters.

2.8. Combining Data from Different Clusters or Datasets

As long as the parameters to be determined can be assumed the same within different clusters or datasets the information can be combined by simply adding the likelihoods found for the individual datasets before searching the best fitting parameters. It is thus possible to combine, for example, a dataset with distance information with a larger one without distance information for a given cluster, even if they were made using different selection criteria or to combine different clusters observed using different selection criteria. Clearly the galaxies within a given dataset must have been chosen randomly from within the redshift, angular separation, and magnitude bins describing that dataset.

If the clusters in question are not "equal", which in general will be the case, it becomes necessary to rescale them before performing the maximum-likelihood analysis. This can be done easily and with good results, as demonstrated by Carlberg et al. (1997b), who studied the virialized regions.

3. RESULTS FOR COMA

We shall now apply the models presented above to the Coma cluster. As mentioned above one should be cautious when using data for one cluster only. Unfortunately, Coma is currently the only cluster for which we have access to the type of data needed for a large part of the infall region.

Since the model includes contributions from background galaxies, but not from other clusters, it is important to select a region of phase space which is not 'contaminated' by other clusters, yet contains as many galaxies belonging to the infall region of Coma and its outskirts as possible and simultaneously is large enough to constrain the sought-after parameters efficiently.

Figure 5 shows Coma viewed in the (cz, θ)-plane. Filled circles are data from *zcat* (Huchra et al 1993) and open triangles are from vH. The rectangle inside the dashed lines defines the region of phase space we decided to model. It is a bit narrower in cz than we would like, but this was done in order to avoid including a significant number of galaxies from the 'filament' extending from the cluster A1367.

The inner cutoff has to be large enough so that virialization and shell crossing have no effect on the galaxies selected. We use $\theta_{low} = 2°$ which corresponds to $r \approx 2.4h^{-1}Mpc$. The outer cutoff is 8°, large enough to contain most of Coma, yet small enough to avoid inclusion of galaxies heavily interacting with the surrounding clusters. The precise values of the two cutoffs are not important, and we have checked this by also running our models with cutoffs at 3° and 10°.

It is well known that Coma is not perfectly spherical and that its early- and late-type galaxies are not distributed similarly. This has been demonstrated convincingly, for example, by Doi et al., (1995). To study the effects of this substructure in Coma on our analysis, we subdivided the dataset in three different ways: firstly into early- and late-type galaxies (according to Hubble type), secondly into inner and outer galaxies (according to θ), and thirdly in high- and low-density regions, according the whether or not the galaxies are near or far from the two filaments (in ϕ) visible in Figure 6. In the latter two cases the cuts were made such that each splitting resulted in approximately the same number of

galaxies in the two parts.

Despite going to much fainter luminosities, there is a distinct drop in the number of galaxies per magnitude bin at 15.5 in the full sample. Therefore, we have made a lower cutoff in luminosity at m=15.5. Furthermore, we decided to ignore the extra data included in the vH sample, as only few of them are found within the region of phase space considered here.

The results are presented in Tables 2 and 3, while Figures 7a – 7c are examples of the likelihood contours found (with symbols as in Figure 4). In Table 2 the left half shows results for the DI model, while the right half are results for the DII model. The fits are for all 143 galaxies in the dataset. The value of Ω_0 shown on the left is the one assumed in the analysis in order to convert a mass profile to a velocity profile. In Table 3 the left half contains results for the VI velocity profile, the right half for the VII velocity profile. The uppermost line gives the result for all 143 galaxies, whereas the results below are for the various subdivisions described above.

We note how robust the estimates of the turn-around radius are to changes in the assumptions concerning Ω_0, σ_{cz}, and the velocity profile. For the total dataset the full range of values returned is $9.0h^{-1}Mpc \leq r_{turn} \leq 10.0h^{-1}Mpc$. Table 2 illustrates the effect of changing σ_{cz}. An increase in σ_{cz} will increase the width of the caustics for a given velocity profile, hence a fixed dataset results in a lower estimate of the systematic infall velocity at a given distance from the cluster.

The only subsets of Coma data which result in a clear change in the velocity profile are the "high-density" galaxies and the "inner" galaxies. These are exactly the subsets that we would expect to deviate *a priori* from the analysis, the high density galaxies because local effects are likely stronger in the dense surroundings and because the marked deviation from our assumption of spherical symmetry (e.g. $n_{gal}(r)$ being spherically symmetric). The inner galaxies deviate because the strongest signal in that region comes from the galaxies falling fastest towards the cluster, thus providing little information towards a determination of the turn-around radius.

3.1. Implications of the Results for Coma

What can we deduce from the Coma results? Firstly, we do not have enough data to arrive at any firm conclusions. The parameters found are not strongly constrained, and working on a single cluster our assumption of sphericity might well break down.

Having said that it should be noted that the velocity profiles found are very similar for a given value of σ_{cz}. Not only is this true among models and cosmologies, interestingly enough it is also the case for the subdivided sets of Coma, with the exception of precisely those sets for which we would expect deviations. It seems our results are not completely arbitrary!

As a further check we can compare the mass estimates provided by our models at a small radius to the virial estimate of the mass of the Coma cluster. This is done in Figure 8, where we plot the estimated masses at $r = 2.5h^{-1}Mpc$ and r_{turn} using the DI profile results. Circles are for $\sigma_{cz} = 300$ km s^{-1}, triangles for $\sigma_{cz} = 400$ km s^{-1}, and filled symbols for the smaller of the two radii. The inner mass estimates are nearly insensitive to the adopted value of Ω_0, as one would expect. The mass estimates at $2.5h^{-1}Mpc$ are around $2 \times 10^{15}h^{-1}M_\odot$ for the low-velocity dispersion models and around $1.5 \times 10^{15}h^{-1}M_\odot$ for the high-velocity dispersion models. Based on X-ray data Hughes (1989) found $M(r \leq 2.5h^{-1}Mpc) = 0.5 - 1.5 \times 10^{15}h^{-1}M_\odot$, with preferred values in the range $M(r \leq 2.5h^{-1}Mpc) = 0.8 - 1.1 \times 10^{15}h^{-1}M_\odot$, while Watt et al. (1992) estimate the total mass to be $1.3 \times 10^{15}h^{-1}M_\odot$. Using galaxy line-of-sight velocities, The & White (1986) find $M(r \leq 2.7h^{-1}Mpc) = 0.3 - 2.5 \times 10^{15}h^{-1}M_\odot$, with a value of $0.95 \times 10^{15}h^{-1}M_\odot$ assuming mass and galaxies are similarly distributed. Colless & Dunn (1996) find $M_{virial} = 0.9 \times 10^{15}h^{-1}M_\odot$. As emphasized by these and other authors, determinations based solely on galaxy velocities yield large uncertainties. Recall that our results do not rely in any way on data from the virialized region (except for providing the center of Coma). The good agreement between our results and the results quoted above is strong evidence that the method works, notwithstanding our "testing" laboratory with its simulated clusters. Performing a similar analysis, but using results found for slightly different cuts in angular selection (3–8°, 2–10°, 3–10°), we find $M(r \leq 2.5h^{-1}Mpc) = 1.1 - 2.4 \times 10^{15}h^{-1}M_\odot$, again indicating that our results are far from accidental.

If we had good knowledge of the luminosity profile of Coma, its M/L ratio as a function of radius could be derived for the whole infall region when combined with our results. Unfortunately, such a profile does not yet exist. vH did a very careful study of the light profile of Coma, using Ca and APM data separately to derive two light profiles, but they are based solely on data from the region $\theta \leq 2°$, making extrapolation to $r_{turn} \approx 10h^{-1}Mpc$ too uncertain.

Alternatively, we attempt to use the luminosity profile, $n_{gal}(r)$, specified in the models. Kent & Gunn (1982) estimated the total luminosity of Coma inside $\theta \leq 3°$ to be $L_B = 4 \times 10^{12}h^{-2}L_\odot$. This value can be used for normalization of our luminosity profile, and we can derive estimates of the total luminosity inside a given radius. As an example,

Figure 9 shows the mass-to-light ratio calculated this way at $r = 2.5h^{-1}Mpc$ and at r_{turn} (filled versus open symbols) for the DI profile for both the low and high value of the velocity dispersion parameter (circles and triangles).

In the slightly non-linear regime one has:

$$\frac{v(r)}{H_0 r} = 1 - \frac{1}{3}\Omega_0^{0.6}\frac{\Delta}{(1+\Delta)^{0.25}}, \tag{20}$$

where Δ is the relative mass over-density (Yahil 1985). That the luminosity does not necessarily follow the mass can be taken care of through a bias parameter: $\Delta_L = b\Delta$. In this case the peculiar velocity scales approximately as $\Omega_0^{0.6}/b^{0.75}$ when Δ_L is substituted directly for Δ in Equation 20, in the outer infall region where the average over-density is larger than one, yet small enough that Equation 20 still provides a good fit to the real non-linear infall solution (see RG Figure 5).

In Figure 10 we show some of the velocity profiles obtained using our model as well a set of curves based upon Equation 20 and using $n_{gal}(r)$ to provide an estimate for Δ_L. The thick solid lines correspond to predicted velocity profiles based on the light profile assuming $\Omega_0^{0.6}/b^{0.75} = 1.0$, 0.8, 0.6, 0.4, and 0.2, where 1.0 is the lowest line. The thin solid lines are from models VI and VII, the thin dashed lines the DI profile for both values of σ_{cz}, and the thin long-dashed lines are for the DI profile as above, but for θ in the $3° - 10°$ interval. From Figure 10 we see that $0.6 < \frac{\Omega_0^{0.6}}{b^{0.75}} < 0.8$, but we caution the reader that the basis for the luminosity profile we use, the cluster-galaxy correlation function, is not necessarily a very precise description of the light profile of Coma throughout the infall region. While it serves in our models as a reasonable luminosity profile (since the models are not very sensitive to this), one should be careful in interpreting variations of the M/L ratio of Coma based on this profile. Also recall that our mass estimates for the inner region were somewhat too high, indicating the estimated infall velocities could be systematically a bit too large.

Currently much work is being done on the relation between cluster profiles and cosmology (e.g. Cole & Lacey 1996, Navarro, Frenk, & White 1997). Nearly all the work, however, applies mainly to the virialized part of the clusters. It would be very useful to extend the work to the infall region, in which case the density profiles derived using models such as those presented here could be compared with results from N-body simulations.

The values of r_{turn} for Coma inferred from our models show little variance. Given some well-defined inner radius (e.g. the virial radius, r_{vir}) or the radius at a given average over-density, one might intuitively expect that the ratio r_{turn}/r_{vir} would allow discrimination between different cosmological models. There is an indication from Figure 5 of Crone et al. (1994) that this may be the case, but it is probably only through future high-resolution N-body simulations that one can hope to answer such a question.

4. DISCUSSION

The main difference between the models presented here and previous attempts to determine the masses of clusters on the basis of their infall velocity profiles is the inclusion of a noise term, which represents the effects of small-scale structure and observational errors, and the use of the full distribution function, $f(cz, \theta, m)$, rather than the caustic envelope, when fitting models to data. Furthermore, our modelling does not rely strongly on the light profile, which is not well determined in the infall region of individual clusters.

Visual inspection reveals that in the limit of a no-noise term the model distribution and the real distributions are dissimilar (Figure 2). With hindsight it is therefore not surprising that RG and vH were unable to decide upon a best-fit model. Had they found one it might have resulted in false conclusions, as the effect of small-scale substructure and observational errors, represented through σ_{cz} in our models, is to increase the apparent width of the caustic surfaces. Without accounting for this effect the inferred systematic velocities become too high.

With the noise term included in our models, the (cz, θ, m) distributions become acceptable to the eye (Figure 2), but as discussed earlier such a smearing of the caustics is also expected from an aspherical infall. Which of the two interpretations is correct? Most likely a combination, as both explanations are based upon known physical effects. It is well known that clusters are not perfectly spherical (see Figure 6 of the Coma cluster) which must result in a systematic flow which is not perfectly radial if the distribution of the dark matter is anywhere near the distribution of the galaxies. On the other hand, galaxies do induce substantial non-radial motions upon one another, even on scales so small that the effect clearly is not accounted for by a non-spherical cluster potential (e.g. in pairs and groups of galaxies) which should be combined with an observational error of the order ~ 100 km s^{-1}. Furthermore, the level of σ_{cz} which leads to models resembling Coma is of the order 300–400 km s^{-1}, which is very close to the observed pairwise velocity dispersion for a single galaxy, which we expect to be a good measure of the "noise" on small scales.

Are the effects of overall non-sphericity, be it a non-spherical potential resulting in a non-radial flow or a radial flow but mainly along a few filaments, so strong that they hamper the use of the spherical infall model, or the use of the particular models presented here? There is no doubt that using the spherical approximation for individual clusters one risks drawing false conclusions, as demonstrated by van Haarlem & van de Weygaert 1993 on N-body data. They found everything from good to poor agreement between a spherical infall solution and the actual radial velocity distribution of the various clusters in their simulations. Thus to model individual clusters one will in general need to go beyond the spherical approximation. An attempt to do that has been made by Diaferio & Geller (1997).

But evidently an ensemble cluster, made by the superposition of a number of clusters, must be spherical. This is found to be the case for clusters in N-body models (van Kampen, 1995). As one does not have spatial 3D information about real clusters, one might worry that selection effects makes an "observed" ensemble cluster non-spherical, but rather elongated along the line of sight. We believe that such problems can be minimized by using an X-ray selected cluster sample. Work is in progress, using the simulations by van Kampen (1995), to quantify to which degree there might be a problem if using an ensemble of clusters selected on the basis of "optical" data.

The ensemble cluster being spherical, the relevant question is whether the systematic flow of the galaxies in the ensemble cluster can be described by the spherical approximation and related to cosmology. Lilje & Lahav (1991) found this to be the case. They compared the predictions of the spherical infall model applied to density peaks in a random Gaussian field to the outcome of N-body simulations and found the analytic models to give a good representation of the density and velocity profiles found in the simulations.

We conclude that models like the ones presented here will work correctly when applied to a few clusters simultaneously. Further evidence comes from the mass estimates of the virial region of Coma produced with our infall method which are fairly close to the estimates produced based on observations of the inner region of Coma.

How superposition of cluster data will effect the best value of σ_{cz} to use in the models is hard to say. On the one hand, one might expect that if non-radial flows are significant in individual clusters it will lead to an increase in the best value to use when considering a superposition. On the other hand, the values of σ_{cz} might be high already. Assume, for example, that deviations from spherical symmetry smear out the infall profile of Coma. Then the fact that our models represents Coma quite well could indicate that the level of σ_{cz} adopted is higher than what corresponds solely to small-scale substructure. Hopefully, future observational work on the level of the pairwise velocity dispersion on small scales can help answer such questions. It is an important parameter in the models, and it should ideally be determined without using the models themselves. For the purpose of these models one needs estimates of $\sigma_{pairwise}$ which excludes the central regions of clusters, as we need the velocity dispersions on small scales in the probably much "colder" infall regions.

The best way to improve the models of the infall region is, we believe, by means of studying N-body simulations with emphasis on this region. As the typical systematic velocities in the infall region can easily be as small at the internal velocity dispersions of galactic dark matter halos particular care has to be taken the problem of identifying "galaxies" and measuring the velocity field of only those becomes critical. Simulations including simplified galaxy formation, like the ones done by van Kampen (1995), seem

an ideal basis for such a study. Potentially N-body models can provide knowledge about eventual systematic effects such as asphericity and about the way in which σ_{cz} might change due to superposition of clusters, or with the position relative to the cluster center. Also, given that we have found that the value of the turn-around radius of Coma is very insensitive to our modelling, it would be of great interest to identify in N-body simulations any systematic relation between the outer properties of clusters (such as the turn-around radius) and the inner properties (parameters which can be determined on the basis of virial estimates or similar) which relate to cosmology.

5.   CONCLUSIONS

We have modelled the velocity field of the infall region of clusters of galaxies by a superposition of a systematic component, which is spherically symmetric and based on the spherical infall approximation, and a noise component, which is isotropic and independent of position in the cluster, which represent the combined effects of small-scale substructure and observational errors. These random velocities are assumed Gaussian and their level described by σ_{cz}. In the models the mass-to-light ratio is allowed to vary freely. Knowing the systematic component one can deduce the velocity and mass profile of the clusters.

For $\sigma_{cz} = 300 - 400$ km s^{-1} our models resemble Coma quite well. This level corresponds to the observed pair-wise velocity dispersion of galaxies on small scales. The effect of the noise term is to smear out the caustic surfaces searched for by previous groups. The models allow calculation of the phase-space density of galaxies expected at any point in the observable (cz, θ, m)-space outside the region of shell crossing. The likelihood of obtaining a given set of data from a particular model and its parameters can be determined. It is demonstrated on simulated data the maximum-likelihood procedure allows one to identify the correct model parameters, even for realistic noise levels and sample sizes.

To avoid the effects of deviations from sphericity and to enhance the likelihood signal, data for a few clusters should be superimposed when applying the model to real observations. This is technically a simple process, but currently sufficient observational data are not available.

The models do not in any way rely on data for the virial region of the clusters, other than providing the center of the clusters. Hence, the model determination of the cluster mass at small radii can be compared to the virial estimates as a test of the method.

Finally, it is demonstrated that the inclusion of distance information of the precision which can be obtained using the Tully-Fisher relation strengthens the likelihood signal

significantly. Potentially this could be used to allow deviation from the assumption of spherical symmetry.

We have applied our models to the only cluster for which we have enough data far out in the infall region, namely Coma. The estimated mass at $r = 2.5h^{-1}Mpc$ falls in the range $1.1 - 2.4 \times 10^{15}h^{-1}M_\odot$, depending on the model and the level of the noise term. Higher σ_{cz} produces a lower mass estimate. We find the turn-around radius, r_{turn}, to be of the order $10h^{-1}Mpc$, which is fairly insensitive to changes in the models, the noise level, and even to subdivision of the data.

Using the cluster-galaxy correlation function to provide an estimate of the light profile, we find for Coma $0.6 < \frac{\Omega_0^{0.6}}{b^{0.75}} < 0.8$, b being the bias parameter: $b\Delta_{mass} = \Delta_{light}$, where Δ is the relative over-density. We hesitate to draw any firm conclusion on the basis of this result, as long as the present analysis was performed on data from only a single cluster.

However, we have demonstrated that the method does indeed work, and it provides a promising way of measuring the infall velocities in the outer regions of clusters. More observations of redshifts in the outskirts of clusters are needed as well as a dedicated study of the properties of the infall region of clusters from N-body simulations.

Table 1a. Fits to Simulated Clusters.

Simulated	σ_{cz} [km s^{-1}]	Fit	σ_{cz} [km s^{-1}]	#clu	#gal/clu	r_{turn} [Mpc]	β or γ
DI	300	DI	300	300	143	9.70±1.69	2.53±0.52
DI	300	DI	300	150	286	9.64±1.17	2.50±0.37
DI	400	DI	400	300	143	9.59±2.05	2.41±0.61
DI	400	DI	400	150	286	9.69±1.41	2.45±0.41
DI	400	DI	300	300	143	9.38±2.73	2.67±0.73
DI	300	DI	400	300	143	9.93±1.50	2.27±0.47
VI	300	VI	300	70	143	9.01±1.65	1.44±0.33
VI	400	VI	400	100	143	8.93±2.29	1.39±0.35
VII	300	VII	300	20	143	9.20±1.23	8.31±2.51
VI	300	VII	300	20	143	9.49±1.80	7.51±3.00
VI	400	VI	300	100	143	8.47±2.73	1.57±0.38
VI	300	VI	400	100	143	9.70±1.73	1.10±0.37

Table 1b. Fits to Simulated Clusters, Including Distance Information.

Simulated	σ_{cz} [km s^{-1}]	Fit	σ_{cz} [km s^{-1}]	#clu	#gal/clu	r_{turn} [Mpc]	β or γ
DI	300	DI	300	300	143	9.51±0.91	2.51±0.33
DI	300	DI	300	150	286	9.52±0.60	2.51±0.23
DI	400	DI	400	300	143	9.33±1.04	2.49±0.38
DI	400	DI	400	150	286	9.41±0.69	2.49±0.25
DI	400	DI	300	300	143	9.43±1.26	2.68±0.41
DI	300	DI	400	300	143	9.37±0.83	2.35±0.31
VI	300	VI	300	70	143	8.99±0.81	1.42±0.17
VI	400	VI	400	100	143	8.78±1.17	1.39±0.23
VII	300	VII	300	20	143	8.89±0.99	8.90±2.38
VI	300	VII	300	20	143	10.40±0.87	5.28±1.31
VI	400	VI	300	100	143	8.95±1.44	1.53±0.25
VI	300	VI	400	100	143	8.56±0.86	1.25±0.21

Table 2. Fits of D1 and D2 to Coma.

Ω_0	$\sigma_{cz}=$ 300 km s^{-1}		$\sigma_{cz}=$ 400 km s^{-1}		$\sigma_{cz}=$ 300 km s^{-1}		$\sigma_{cz}=$ 400 km s^{-1}	
	γ	r_{turn} $[Mpc\ h^{-1}]$	γ	r_{turn} $[Mpc\ h^{-1}]$	γ	r_{turn} $[Mpc\ h^{-1}]$	γ	r_{turn} $[Mpc\ h^{-1}]$
0.01	2.8	9.5	2.5	10.0	2.8	9.5	2.5	10
0.2	2.6	9.5	2.4	10.0	2.8	9.0	2.5	9.5
0.4	2.5	9.5	2.3	10.0	2.6	9.0	2.4	9.5
0.7	2.5	9.5	2.2	10.0	2.7	8.5	2.4	9.0
1.0	2.4	9.5	2.2	10.0	2.6	8.5	2.3	9.0

Table 3. Fits of V1 and V2 to Coma.

Component	θ degrees	N	r_{turn} $[Mpc\ h^{-1}]$	β	r_{turn} $[Mpc\ h^{-1}]$	β $[Mpc\ h^{-1}]$
All	2-8	143	9.5	1.6	10.0	9.0
Early types	2-8	51	9.0	1.7	10.0	8.0
Late types	2-8	92	10.0	1.7	10.5	10.5
High density	2-8	74	13.5	1.4	14.0	7.0
Low density	2-8	69	9.5	1.4	10.0	6.5
Inner region	2-5	73	8.0	2.0	8.5	12.0
Outer region	5-8	70	10.5	2.0	10.5	12.0

REFERENCES

Carlberg, R.G., Yee, H.K.C., Ellingson, E., Morris, S.L., Gravel, P., Pritchet, C.J., Smecker-Hane, T., Hartwick, F.D.A., Hesser, J.E., Hutchings, J.B., & Oke, J.B. 1997a, ApJ, 485, 13L

Carlberg, R.G., Yee, H.K.C., Shepherd, C.W., Gravel, P., Ellingson, E., Morris, S.L., Schade, D., Hesser, J.E., Hutchings, J.B., Oke, J.B., Abraham, R., Balogh, M., Wirth, G., Hartwick, F.D.A., Pritchet, C.J., & Smecker-Hane, T. 1997b, (astro-ph/9704060)

Cole, S. & Lacey, C. 1996, MNRAS, 281, 716

Colless, M. & Dunn, A.M. 1996, ApJ, 458, 435

Crone, M.M., Evrard, A.E., & Richstone, D.O. 1994, ApJ, 434, 402

David, L.P., Jones, C., & Forman, W. 1995, ApJ, 445, 578

Davis, M. & Peebles, P.J.E. 1977, ApJS, 34, 425

Dekel, A., Burstein, D., & White, S.D.M. 1996, to appear in "Critical Dialogues in Cosmology", ed. N. Turok, Princeton 250th Anniversary, (World Scientific)

Diaferio, A. & Geller, M.J. 1997, ApJ, 481, 633

Doi, M., Fukugita, M., Okamura, S., & Turner, E.L. 1995, AJ, 109, 1490

Fisher, P. & Tyson, J.A. 1997, AJ, in press

Huchra, J.P., Geller, M.J., Clemens, C.M., Tokarz, S.P., & Michel, A. 1993, the CfA Redshift Catalogue, unpublished (*zcat*)

Hughes, J.P. 1989, ApJ, 337, 21

Kaiser, N. 1987, MNRAS, 227, 1

Kent, S. M. & Gunn, J.E. 1982, AJ, 87, 945

Lilje, P. B. & Efstathiou, G. 1988, MNRAS, 231, 635

Lilje, P. B. & Lahav, O. 1991, ApJ, 374, 29

Marzke, R.O., Geller, M.J., da Costa, L.N., & Huchra, J.P. 1995, AJ, 110, 477

Narvarro, J.F., Frenk, C.S., & White, S.D.M. 1997, ApJ, submitted (astro-ph/9611107)

Peebles, P.J.E. 1980, "The Large-Scale Structure of the Universe" (Princeton: Princeton University Press)

Regös, E. & Geller, M.J. 1989, AJ, 98, 755 (RG)

Silk, J. 1977, A&A, 59, 53

Smail, I., Ellis, R.S., Dressler, A., Couch, W.J., Oemler, A.Jr., Sharples, R.M., & Butcher, H. 1997, ApJ, 479, 70

Squires, G., Neumann, D.M., Kaiser, N., Fahlman, G., Woods, D., Babul, A., & Böringer, H. 1996, ApJ, 469, 73

The, L.S. & White, S.D.M. 1986, AJ, 92, 1248

Tyson, J.A. & Fisher, P. 1995, ApJ, 446, 55L

van Haarlem, M.J., Cayón, L., de la Cruz, C.G., Martínez-González, E., & Rebolo, R. 1993, MNRAS, 264, 71 (vH)

van Haarlem, M. & van de Weygaert, R. 1993, ApJ, 418, 544

van Kampen, E. 1994, "Formation and Evolution of Clusters of Galaxies and Voids", (Leiden, PhD-thesis)

Watt, M.P., Ponman, T.J., Bertram, D., Eyles, C.J., Skinner, G.K., & Willmore, A.P. 1992, MNRAS, 258, 738

Willick, J.A., Courteau, S., Faber, S.M., Burstein, D., Dekel, A., & Strauss, M.A. 1997, ApJS, 109, 333

Yahil, A. 1985, in "The Virgo Cluster of Galaxies", eds. O.G. Richter & B. Binggeli, (European Southern Observatory: Garching bei München)
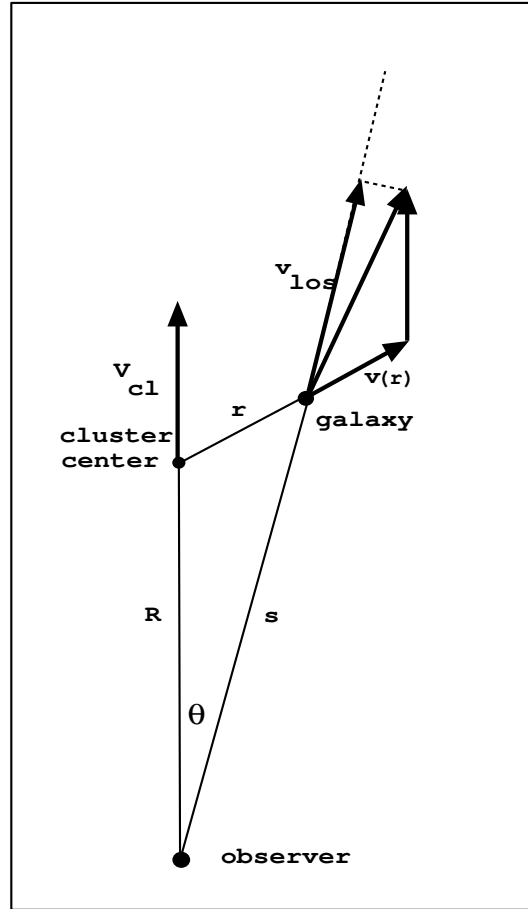
Fig. 1.— A diagram showing how the various geometrical quantities in the models are defined.
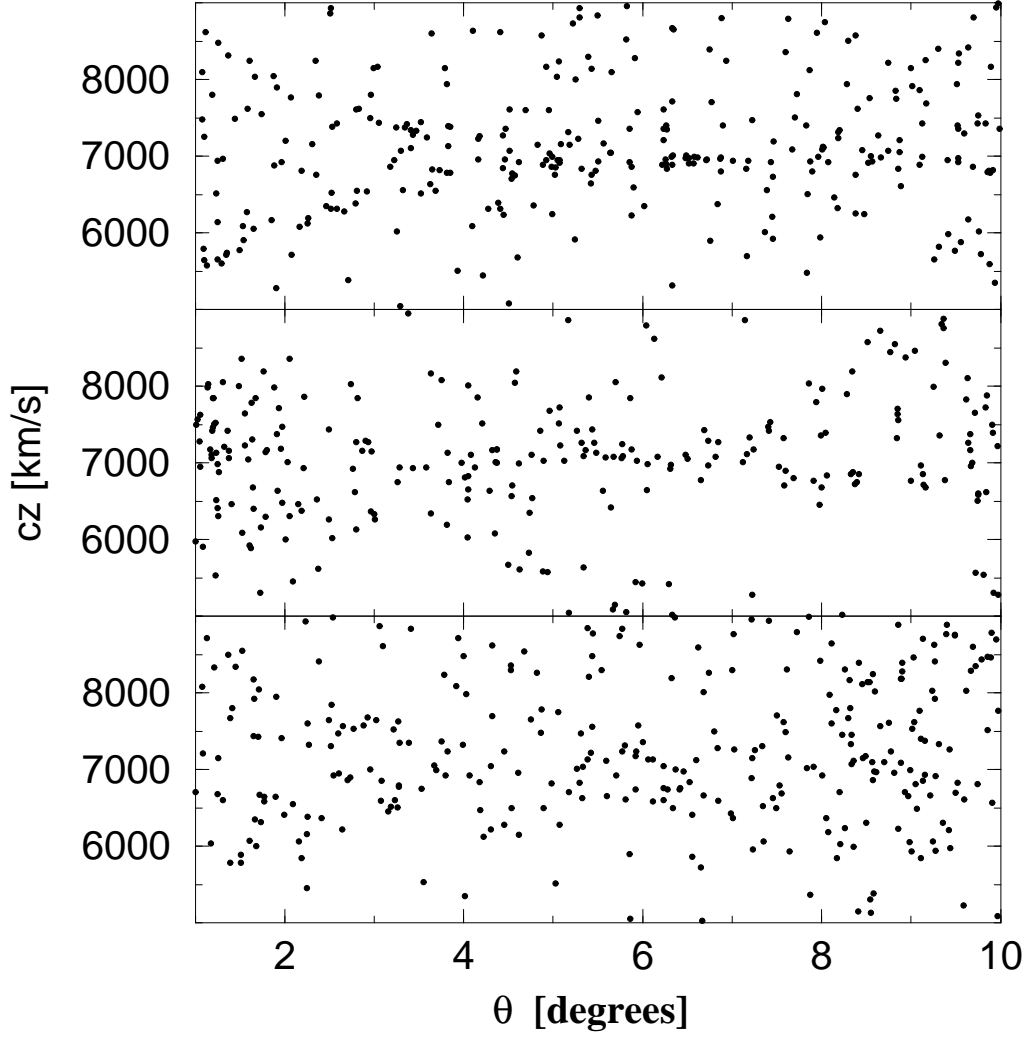
Fig. 2.— (θ, cz) diagrams of, (a) model based on profile VI with $r_{turn} = 9, \beta = 1.4$ and no smearing term (Equation 12 but including magnitude term as in Equation 16), (b) Coma in similar diagram (only galaxies having apparent magnitude < 15.5), and (c) as (a) but now including a smearing term in cz of strength $\sigma_{cz} = 300$ km s^{-1} (Equation 16).
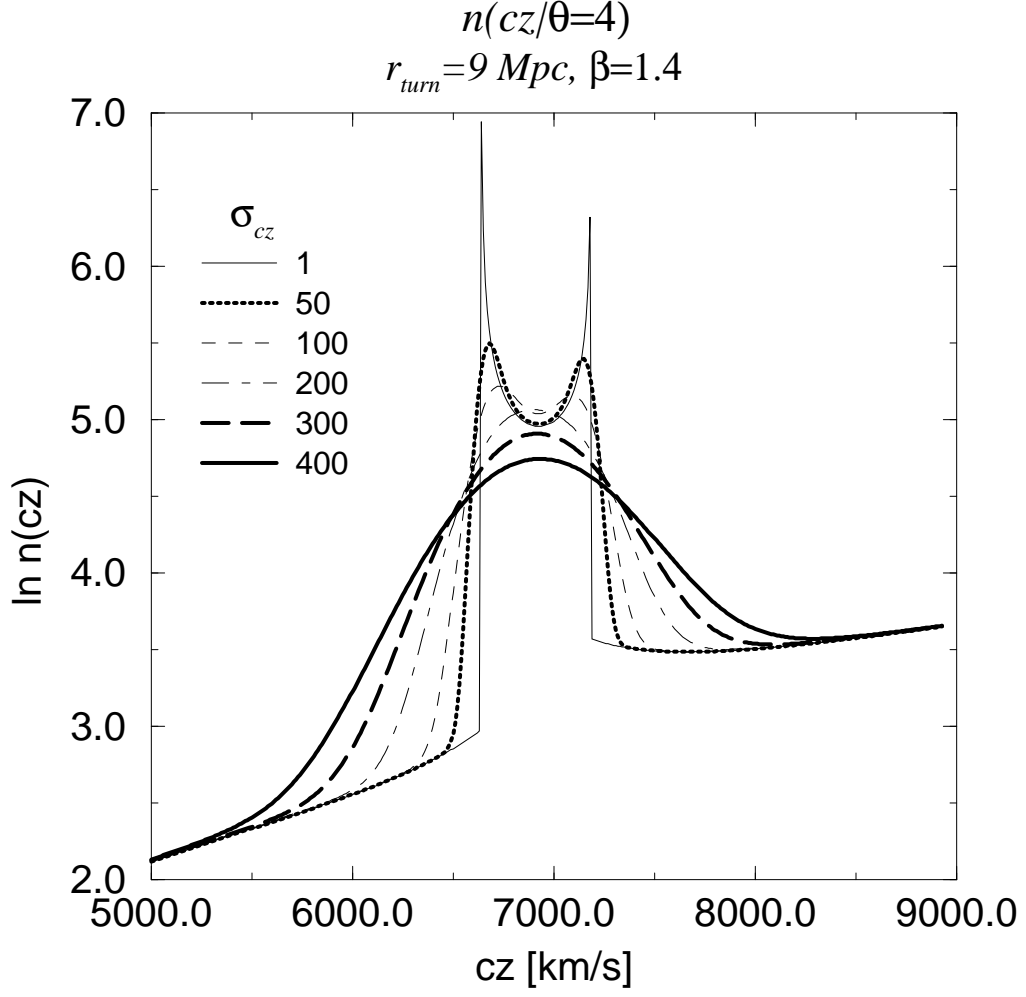
Fig. 3.— $n(cz|\theta, \sigma_{cz})$ curves for $\theta = 4°$ and different values of σ_{cz}.
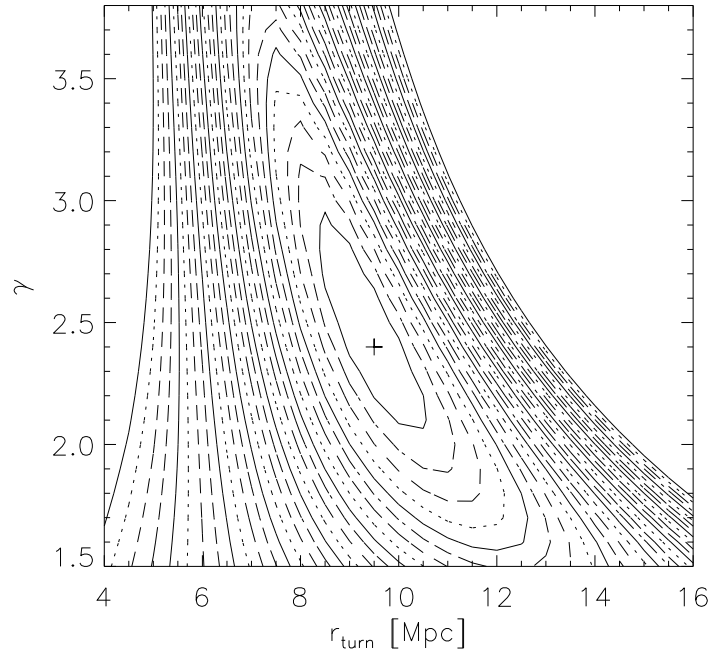
Fig. 4.— Likelihood contours for a simulated cluster constructed using model DI with $\gamma = 2.5$, $r_{turn} = 9.5$, and $\Omega_0 = 0.4$. The cluster contains 143 galaxies and was analysed assuming model DI with $\Omega_0 = 0.4$. Shown is ln(L), and contours are separated by ln(2), maximum is indicated by cross and contours are constantly decreasing moving away from maximum.
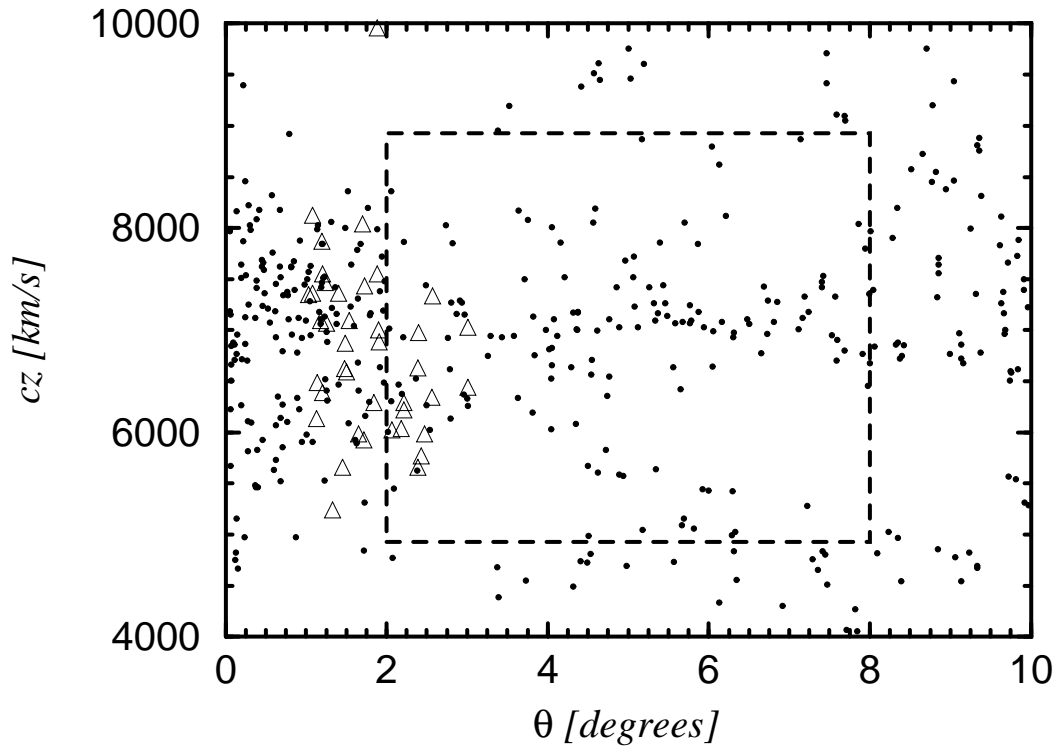
Fig. 5.— (θ, cz) diagrams of Coma, including data from both *zcat* and vH. Region surrounded by dashed lines is the one selected for maximum-likelihood analysis. See text for details.
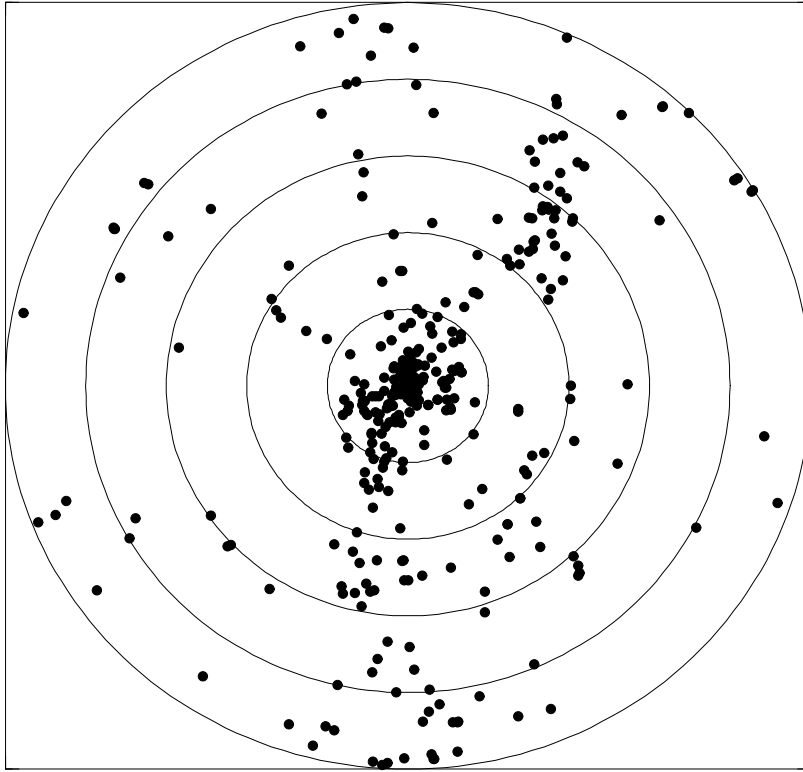
Fig. 6.— Projected view of Coma. Plotted is $(\theta\cos(\phi), \theta\sin(\phi))$ for the same galaxies as shown the previous figure.
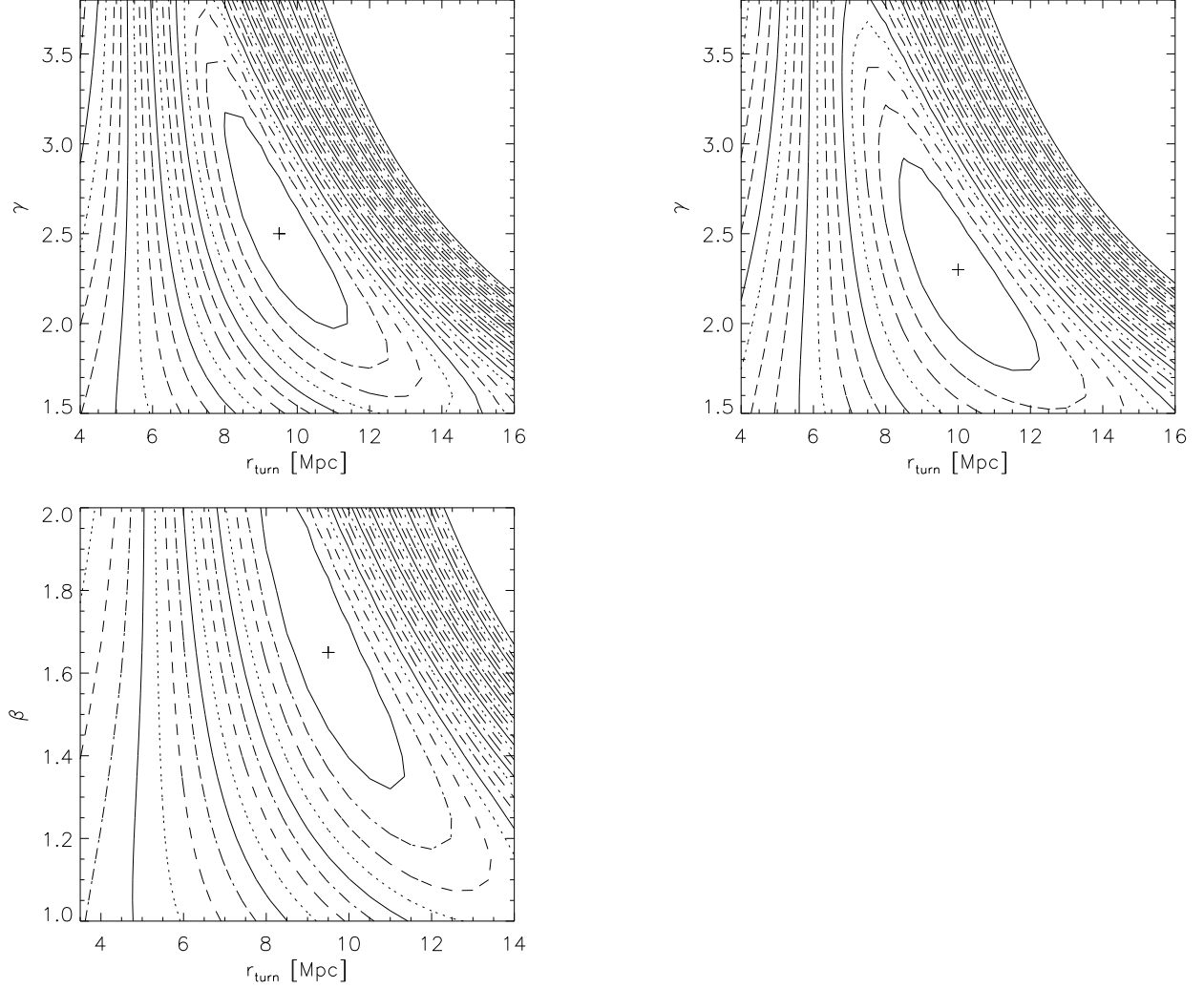
Fig. 7.— Likelihood contours for Coma. Shown is ln(L) and contours are separated by ln(2), maximum is indicated by cross and contours are constantly decreasing moving away from maximum. (top left) assuming model DI, $\sigma_{cz} = 300$ km s^{-1}, and $\Omega_0 = 0.4$, (topright) DI profile and assuming $\sigma_{cz} = 400$ km s^{-1}, and $\Omega_0 = 0.4$, (bottum) VI profile and assuming $\sigma_{cz} = 300$ km s^{-1}.
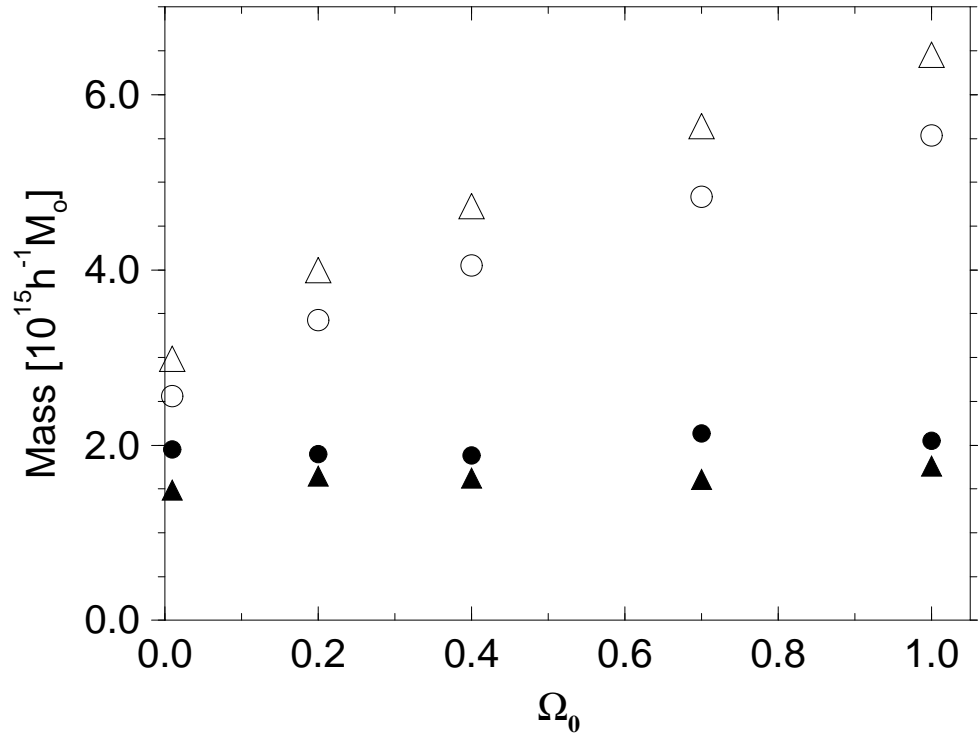
Fig. 8.— Mass estimates at $r = 2.5h^{-1}Mpc$ and r_{turn} of Coma based on the DI models. Filled symbols at lower radius, circles for $\sigma_{cz} = 300$ km s^{-1}, triangles for $\sigma_{cz} = 400$ km s^{-1}.
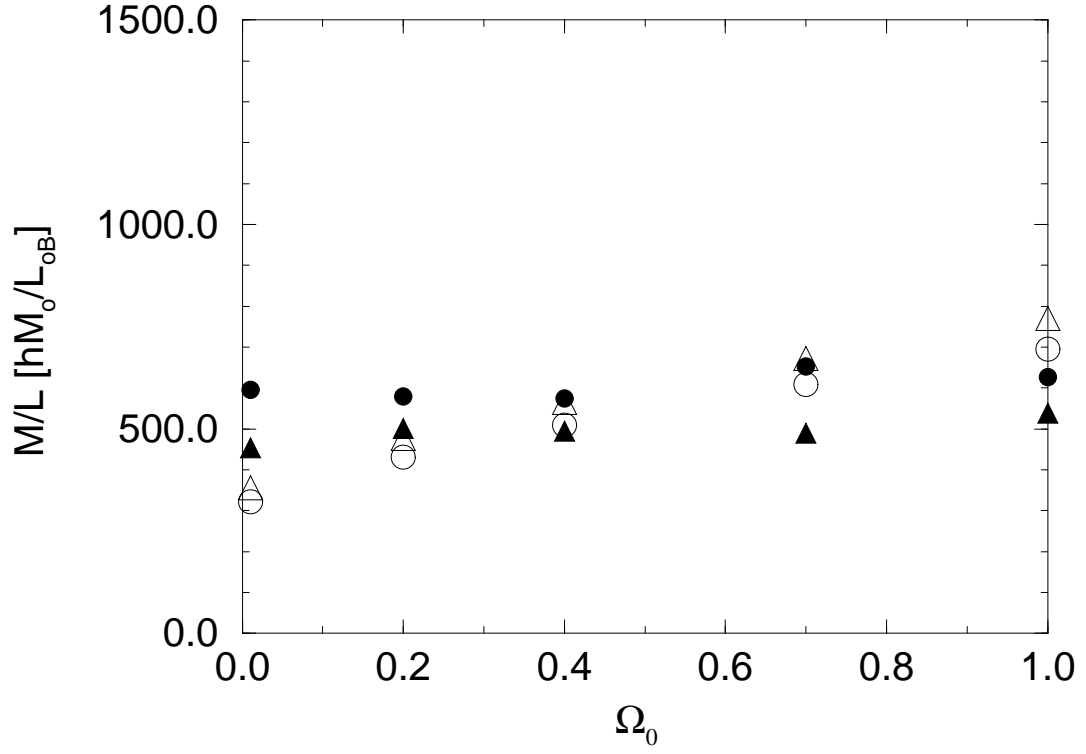
Fig. 9.— Mass-to-light ratio at $r = 2.5h^{-1}Mpc$ and r_{turn} for model DI as function of Ω_0 and assuming $\sigma_{cz} = 300$ km s^{-1} (filled and open circles) and $\sigma_{cz} = 400$ km s^{-1} (filled and open triangles).
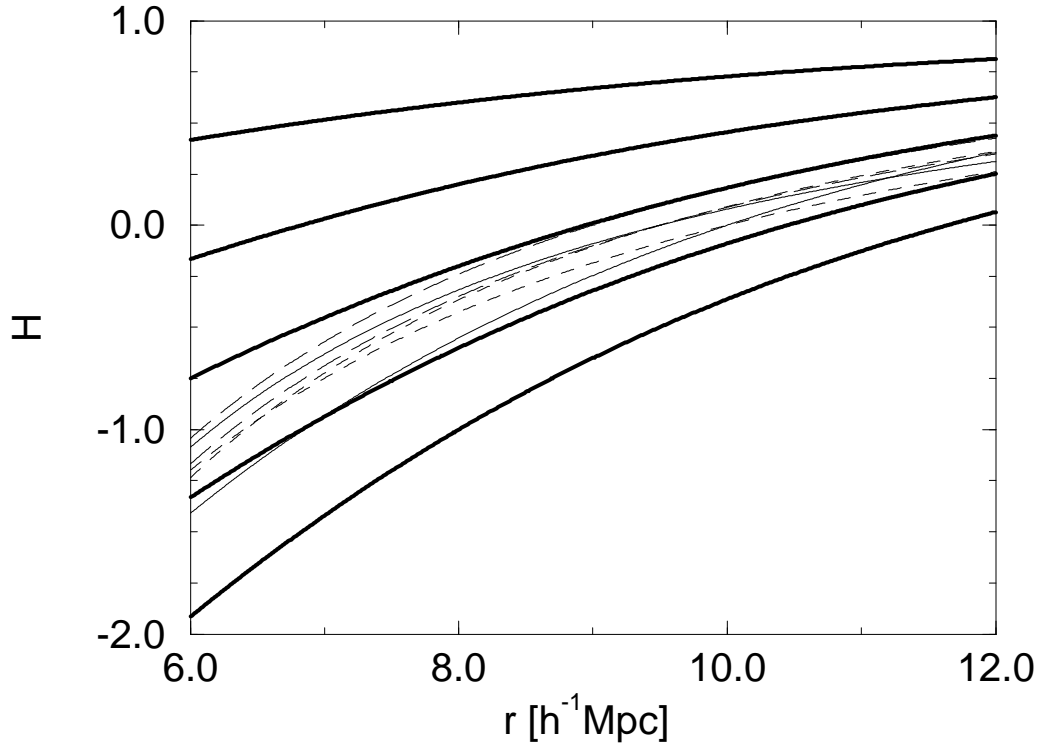
Fig. 10.— Velocity profiles from the models (thin lines) and estimates based on the light profile, assuming $\Omega^{0.6}/b^{0.75} = 1.0$, 0.8, 0.6, 0.4, and 0.2 (thick lines, starting from below). See text for details.